Optical Effects of Energy Terms Linear in Wave Vector*

G. D. MAHAN† AND J. J. HOPFIELD
Department of Physics, University of California, Berkeley, California
(Received 30 January 1964)

Energy terms linear in wave vector are allowed in the second valence band of CdS. Perturbation theory shows that excition states formed with holes from this band will also have a linear splitting. The effect of such terms on the optical properties are discussed using a spatial dispersion approach. Previous reflectivity experiments have some anomalous structure which is shown to be caused by the linear term. Comparing theory with these experiments provides an estimate of these linear terms, which have not been previously measured.

I. INTRODUCTION

SOME crystal symmetry groups allow energy terms which are linear in wave vector. These low-symmetry crystals must lack an inversion center. The linear terms appear as $\pm Ak$, and for finite wave vector, they split a state which is degenerate at $k=0$. Zincblende[1] and wurtzite[2–4] are two examples, and there has been much past speculation[5] on the possible effects of such splittings in semiconductors with these crystal groups. This article presents evidence of such terms in wurtzite CdS, and shows their effect on some optical properties.

The conduction band and three principal valence bands of CdS are shown in Fig. 1. Excitons formed with holes from the different valence band are described as A, B, and C series, respectively. Each band is doubly degenerate at $k=0$. Bands with Γ_7 symmetry, such as the conduction band, allow linear terms for wave vectors perpendicular to the uniaxial (z) axis. In the conduction band,[4] such terms are believed to be absent or at least negligibly small. They may also exist in the lower two valence bands, and their existence there explains the unusual reflectivity measurements on excitons states whose holes are from these bands.[6] The attempt to understand the origin of the anomalous structure of the reflectivity curves was the motivation for examining the effects of the linear terms.

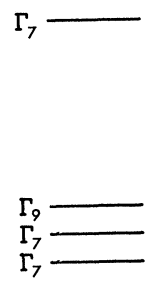

FIG. 1. The symmetries of the conduction band and the three principle valence bands of wurtzite crystals, such as CdS.

Figure 2 shows the measured reflectivities[6,7] of the principal B series exciton state in CdS. Of the three different experimental geometries, only $k\perp z$ and $E\perp z$ shows the extra shoulder of interest. This anomaly has three principal characteristics:

(1) It appears near the transverse frequency. Contrast this with the extra peaks in the A series exciton[6] spectra, which appear at the longitudinal frequency, and are caused by surface effects. This fact suggests that the explanation for the two phenomena are quite different.

(2) The structure is only observed for $k\perp z$, and not for $k\|z$. For $E\perp z$, the $k\rightarrow 0$ symmetry of the $1s$ exciton states for $k\perp z$ and $k\|z$ is the same, Γ_5. The existence of the linear splitting for $k\perp z$, but not for $k\|z$, easily explains this observed directional dependence.

(3) When $k\perp z$, the structure is observed for $E\perp z$ (Γ_5), but not for $E\|z$ (Γ_1). Both transitions are allowed by group theory, and both modes of polarization form $1s$ exciton states which are easily observed in good crystals. This polarization effect, which was originally a puzzling feature, is explained in Sec. II. The linear wave terms mix the Γ_1 state with the longitudinal exciton,[8] which eliminates the linear wave vector term in the energy of this state. The theory of exciton states in CdS, including the effects of linear wave vector terms, is developed in the next section.

In Sec. III, the reflectivity is calculated using the spatial dispersion formulation of Pekar.[9] The nonlocal effects are included using an extension of the classical interpretation which has been recently suggested.[6] The split exciton band is simply represented by two polarization waves. The optical properties of the exciton state

* Research supported by the National Science Foundation. Based in part upon a Ph.D. thesis submitted to the University of California, Berkeley, California.

† Present address: General Electric Research Laboratory, Schenectady, New York.

[1] G. Dresselhaus, Phys. Rev. **100**, 580 (1955).

[2] R. C. Casella, Phys. Rev. Letters **5**, 371 (1960); Phys. Rev. **114**, 1514 (1959).

[3] M. Balkanski and J. des Cloizeaux, J. Phys. Radium **21**, 825 (1960).

[4] J. J. Hopfield, J. Appl. Phys. Suppl. **32**, 2277 (1961).

[5] R. G. Wheeler and J. O. Dimmock, Phys. Rev. **125**, 1805 (1962).

[6] J. J. Hopfield and D. G. Thomas, Phys. Rev. **132**, 563 (1963); **122**, 35 (1961).

[7] D. G. Thomas (private communication).

[8] J. J. Hopfield and D. G. Thomas, Phys. Chem. Solids **12**, 276 (1960).

[9] S. J. Pekar, Zh. Eksperim. i Teor. Fiz. **33**, 1022, 1056 (1957) [English transl.: Soviet Phys.—JETP **6**, 785, 813 (1958)]; Fiz. Tverd. Tela **4**, 1301 (1962) [English transl.: Soviet Phys.—Solid State **4**, 953 (1962)].

are accounted for by having three independent propagating modes in the crystal, each characterized by a different refractive index. In a local theory there would only be one mode.

The effective mass of the B valence band are needed to calculate the reflectivity. These have not been measured, but may be estimated from a knowledge of the A-band masses, which is done in the Appendix.

II. B-SERIES EXCITONS

In wurtzite structures such as CdS, each valence and conduction band is doubly degenerate at $k=0$. In the $\mathbf{k}\cdot\mathbf{p}$ perturbation calculation to determine the effective masses of a band, the only off-diagonal elements in the two-dimensional matrices are terms linear in wave vector.[2–4] Since these were found not to be important for A-series excitons,[4] the optical theory could be formulated using a scalar Hamiltonian.[6] This simplification is one reason why exciton theory in CdS has been able to be developed extensively. For B- and C-series excitons, these off-diagonal terms must be included, requiring use of the matrix formulation.

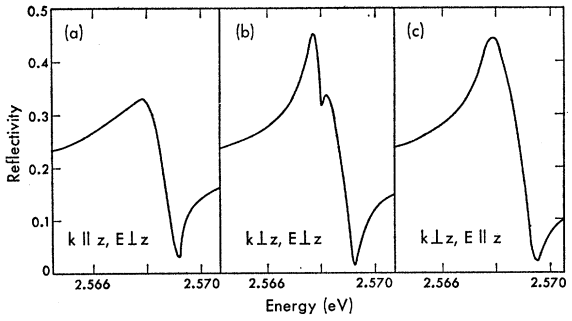

FIG. 2. The reflection spectra of the 1s B series exciton in a single sample of CdS from Hopfield and Thomas. (a) $k\|z$, $E\perp z$, (b) $k\perp z$, $E\perp z$, (c) $k\perp z$, $E\|z$; only (b) shows effect.

Electrons in the conduction band have the wave function

$$\Psi(\mathbf{r})=\sum_{\mathbf{k},j} B_j(\mathbf{k})\psi_{\mathbf{k}}{}^j(\mathbf{r}), \tag{2.1}$$

where $\psi_{\mathbf{k}}(\mathbf{r})$ are the Bloch functions, and the $B_j(k)$ satisfy

$$H_e(k)_{ij}B_j(k)=(\lambda-E_g)B_i(k), \tag{2.2}$$

$$H_e(k)=\begin{pmatrix}(\hbar^2/2m_{e\perp})(k_x{}^2+k_y{}^2)+(\hbar^2/2m_{e\|})k_z{}^2 & c(k_x+ik_y)\\ c(k_x-ik_y) & (\hbar^2/2m_{e\perp})(k_x{}^2+k_y{}^2)+(\hbar^2/2m_{e\|})k_z{}^2\end{pmatrix}. \tag{2.3}$$

There are two independent eigenfunctions $B_j(k)$ which satisfy (2.2) and (2.3), giving two-electron wave functions in (2.1). The eigenvalues of (2.3) are easily found by diagonalization

$$\lambda=E_g+(\hbar^2/2m_{e\perp})(k_x{}^2+k_y{}^2)+(\hbar^2/2m_{\|})k_z{}^2 \pm C(k_x{}^2+k_y{}^2)^{1/2}. \tag{2.4}$$

For wave vectors perpendicular to the z axis,

$$k_\perp=(k_x{}^2+k_y{}^2)^{1/2},$$

the conduction band may exhibit a linear splitting at $k_\perp\to 0$. But measurements indicate that no splitting exists in the conduction band,[4] and C is zero, or small enough to be neglected.

The $\mathbf{k}\cdot\mathbf{p}$ Hamiltonian for the top valence band, which has a different group symmetry, lacks the off-diagonal terms. Only the quadratic terms in (2.4) are present. When discussing excitons from this band, the resulting four-dimensional matrix Hamiltonians has four equal diagonal elements. These are the sum of the diagonal term of (2.3) for the conduction and valence bands plus the Coulomb interaction terms. This Hamiltonian has been analyzed in detail.[6] One choice of center-of-mass coordination allows the diagonal Hamiltonian H_d to be expressed as an isotropic part H_0 plus an anisotropic correction H_1, $H_d=H_0+H_1$. H_0 may be viewed as the unperturbed Hamiltonian, and its eigenstates are hydrogenic, characterized by an average dielectric constant $\epsilon_0=(\epsilon_\perp\epsilon_\|)^{1/2}$ and an average effective mass $\mu_0{}^{-1}=\frac{2}{3}\mu_\perp{}^{-1}+\frac{1}{3}\mu_\|{}^{-1}$. H_1 has as a factor an anisotropy constant γ,

$$\gamma=\mu_0[\mu_\perp{}^{-1}-(\epsilon_\perp/\epsilon_\|)\mu_\|{}^{-1}].$$

Since γ is small ($\gamma\sim 0.2$ for A series, $\gamma\sim 10^{-2}$ for B series[10]), the choice of center-of-mass coordinates is justified, and the ground-state wave functions will be hydrogenic.

The lower two valence bands have the same irreducible representation as the conduction band, and their $k\cdot p$ Hamiltonian must be similar to (2.3), with just different constants $m_{h\perp}$, $m_{h\|}$, and C. Postulating that the energy terms linear in wave vector are small compared to exciton binding energies, the off-diagonal terms in the exciton Hamiltonian matrix may be treated as a perturbation. This causes a linear splitting in the exciton Hamiltonian, and mixes the exciton state.

A suitable set of eigenstates must be chosen in order to represent the four-dimensional matrix. The two s-like conduction-band states may be identified by just the spin, α_c and β_c. Approximate eigenfunctions were previously obtained for the hole bands.[11] The wurtzite valence band structure near $k=0$ may be approximated

[10] See Appendix.
[11] J. J. Hopfield, Phys. Chem. Solids **15**, 97 (1960).

by introducing spin-orbit interaction and a (111) strain into a zincblende valence band. Perturbation theory then relates the wave functions of the three bands. The top band are $J=\frac{3}{2}$, $M_J=\pm\frac{3}{2}$ states. The states for the B band are

$$|\lambda_B,+\rangle=N_B[(2-3\lambda_B/\delta)z\alpha_h-(x+iy)\beta_h],$$
$$|\lambda_B,-\rangle=N_B[(2-3\lambda_B/\delta)z\beta_h+(x-iy)\alpha_h], \quad (2.5)$$
$$N_B=[2+(2-3\lambda_B/\delta)^2]^{-1/2}.$$

The C band is the same as (2.5), with λ_C replacing λ_B. The measured energy splittings of the bands beneath the A band[12] are $\lambda_B=0.016$ eV and $\lambda_C=0.073$ eV, and the spin-orbit splitting is $\delta=0.060$ eV. Only excitons from the B band are sufficiently resolved to allow the effect of the linear term to be observed in optical experiments. Since the lower two valence bands have identical group symmetry, the same calculation applies to either band. In principle, the C band should show the same effects. The two states of a valence band will be labeled $|\pm\rangle$, and the results apply to either the B or C band.

The symmetry of the exciton states is found from the product of the representations of the conduction band (Γ_7), the valence band (Γ_7), and the hydrogenic state. Only the $1s$ hydrogenic state is easily observed optically, and its symmetry (Γ_1) will be used. $\Gamma_1\times\Gamma_7\times\Gamma_7=\Gamma_1+\Gamma_2+\Gamma_5$. The Γ_5 representation is two dimensional. The four exciton states forming a possible basis of the matrix Hamiltonian are

$$\Gamma_5: \quad \begin{pmatrix}\alpha_C|+\rangle\\ \beta_C|-\rangle\end{pmatrix}, \quad (2.6)$$

$$\Gamma_1: \quad (1/\sqrt{2})[\alpha_C|-\rangle+\beta_C|+\rangle],$$
$$\Gamma_2: \quad (1/\sqrt{2})[\alpha_C|-\rangle-\beta_C|+\rangle]. \quad (2.7)$$

The interesting effects occur for wave vector components perpendicular to the z axis. For simplicity we set $k_z=0$, and worry only about the principal geometries of $E\|z$ and $E\perp z$. For $k\perp z$, the Γ_5 has a transverse (Γ_{5T}) and a longitudinal (Γ_{5L}) state. The optical dipole transitions allowed by group theory are to Γ_{5T} ($E\perp z$) and $\Gamma_1(E\|z)$. The reduction of the Γ_5 state to its longitudinal and transverse components depends upon wave vector direction. Select $k=k_y$, but the results will apply to any wave vector in the (x,y) plane

$$\Gamma_{5T}: \quad (1/\sqrt{2})[\alpha_C|+\rangle-\beta_C|-\rangle],$$
$$\Gamma_{5L}: \quad (1/\sqrt{2})[\alpha_C|+\rangle+\beta_C|-\rangle]. \quad (2.8)$$

The four states (2.7) and (2.8) are chosen as the basis for the excitons matrix Hamiltonian. It is convenient to use the ordering ψ_2, ψ_{5T}, ψ_{5L}, ψ_1.

$$H_{\text{exciton}}=\begin{bmatrix}H_d & V & 0 & 0\\ V & H_d & 0 & 0\\ 0 & 0 & H_d+\Delta & V\\ 0 & 0 & V & H_d\end{bmatrix}, \quad (2.9)$$

[12] D. G. Thomas and J. J. Hopfield, Phys. Rev. **116**, 573 (1960).

V is the off-diagonal term from the valence band which is linear in wave vector,

$$V=\varphi k_\perp, \quad (2.10)$$
$$\varphi=Cm_{h\perp}/(m_{e\perp}+m_{h\perp}). \quad (2.11)$$

φ is the exciton splitting parameter. Here only the center-of-mass part of V has been retained, and the exciton relative coordinate parts have been set equal to zero. These relative terms will mix the $1s$ state with other hydrogenic levels,[4] but these effects are not important here. The additional term Δ in (2.9) represents the splitting of the longitudinal exciton[8] above the transverse state. Long-range Coulomb interaction raises its resonance frequency above that of the transverse state, and this may be represented by the diagonal constant Δ in this basis.

The linear interaction V mixes the ψ_2 and ψ_{5T} states

$$\mathcal{E}_\pm=\mathcal{E}_0(K)\pm\varphi K_\perp, \quad \psi_\pm=(1/\sqrt{2})(\psi_{5T}\pm\psi_2), \quad (2.12)$$
$$\mathcal{E}_0(K)=\mathcal{E}_0(0)+\hbar^2K_\perp^2/2m_\perp.$$

The ψ_{5L} and ψ_1 states are also mixed, with eigenvalues

$$\mathcal{E}_\pm'=\mathcal{E}_0(K)+(\Delta/2)\pm[(\Delta/2)^2+\varphi^2K_\perp^2]^{1/2}. \quad (2.13)$$

The constant φ is small ($\sim10^{-9}$ eV-cm) and $\Delta\sim10^{-3}$ eV; for wave vectors of interest, $K_\perp\sim10^5$ cm^{-1}, so that $\Delta\gg\varphi K_\perp$. To lowest powers in $K_\perp/\Delta$, the states are

$$\mathcal{E}_+'\approx\mathcal{E}_0(K)+\Delta+\varphi^2K_\perp^2/\Delta, \quad \psi_+'\approx\psi_{5L}+\psi_1\varphi K_\perp/\Delta,$$
$$\mathcal{E}_-'\approx\mathcal{E}_0(K)-\varphi^2K_\perp^2/\Delta, \quad \psi_-'\approx\psi_1-\psi_{5L}\varphi K_\perp/\Delta. \quad (2.14)$$

Because the longitudinal-transverse exciton splitting is so large, the states ψ_1 and ψ_{5L} do not mix appreciably, and neither has a linear splitting. Consider the two allowed transitions: For $E\perp z$, the exciton band will be linearly split at $K_\perp=0$; for $E\|z$, there is no linear splitting. This is what is observed experimentally. It should be emphasized that the results (2.12), (2.13), and (2.14) are true for any wave vector in the (k_x,k_y) plane.

For $k\perp z$ and $E\|z$, (2.14) shows that the linear term does contribute to the exciton mass. The energy is ($k_z=0$)

$$\mathcal{E}'=\mathcal{E}_0(0)+\frac{\hbar^2k_\perp^2}{2}\left[\frac{1}{m_\perp}-\frac{2\varphi^2}{\Delta\hbar^2}\right].$$

The quantity $\hbar^2\Delta/2\varphi^2\sim1.3\times10^{-27}$ g, so that the resulting mass correction is appreciable. This surprising result implies that for $k\perp z$, the exciton mass in the lower valence band depends upon the polarization of the exciting electromagnetic field. If this difference could be detected experimentally, it would provide the most direct method of measuring the linear crossing constant.

III. REFLECTIVITY

The ordinary local theory of optical experiments is inadequate in calculating the reflectivity of this system.

Instead, one must use the spatial dispersion theory introduced by Pekar. Here a separate polarization wave is associated with each of the two components of the split exciton band. At optical frequencies near the resonance frequency both polarization modes are important. When the coupling to the electromagnetic field is introduced, three independent modes of propagating energy result.

The refractive indices for the three modes are found easily by a classical analysis. Label the two polarization modes $P_\pm$.

$$\frac{1}{C^2}\frac{\partial^2}{\partial t^2}[\epsilon_0 E+4\pi(P_++P_-)]=\frac{\partial^2}{\partial x^2}E, \tag{3.1}$$

$$\left[\mathcal{E}_\pm\left(\frac{\hbar}{i}\frac{\partial}{\partial x}\right)^2+\hbar^2\frac{\partial^2}{\partial t^2}\right]P_\pm=\beta_\pm\mathcal{E}(0)^2E, \tag{3.2}$$

$$\mathcal{E}_\pm(k_x)=\mathcal{E}(0)+(\hbar^2k_x^2/2m)\pm\varphi k_x. \tag{3.3}$$

Since only the leading terms of k are important in (3.2) set

$$\mathcal{E}_\pm(k_x)^2=\mathcal{E}(0)^2+2\mathcal{E}(0)[(\hbar^2k_x^2/2m)\pm\varphi k_x]. \tag{3.4}$$

Defining β_0 as the polarizability constant for the exciton band for $\varphi=0$, then $\beta_0=\beta_+/2=\beta_-/2$. This follows from the definition of β_0 as proportional to the square of a matrix element

$$\beta_\pm\alpha|\langle\psi_\pm|H'|0\rangle|^2,$$

and from (2.12) for $\psi_\pm$; H' is the transverse electromagnetic interaction.

For a plane solution, with $P_\pm$, $E\sim\exp(i\omega/c)(nx-ct)$, (3.1) and (3.2) become

$$\begin{aligned}
&n^2-\epsilon_0=\frac{b}{2}\left(\frac{1}{n^2-\mu+an}+\frac{1}{n^2-\mu-an}\right),\\
&b=4\pi\beta_0[mc^2\mathcal{E}(0)/\hbar^2\omega^2],\\
&\mu=-\left[\frac{mc^2\mathcal{E}(0)}{\hbar^2\omega^2}\right]\left\{1-\left[\frac{\hbar\omega}{\mathcal{E}(0)}\right]^2-i\Gamma\frac{\hbar\omega}{\mathcal{E}(0)^2}\right\},\\
&a=(2mc^2/\hbar^2c\omega)\varphi.
\end{aligned} \tag{3.5}$$

Now (3.5) is a cubic equation for n^2,

$$\begin{aligned}
n^6-n^4(\epsilon_0+2\mu+a^2)+n^2[\epsilon_0(2\mu+a^2)+\mu^2-b]\\
-\mu(\epsilon_0\mu-b)=0,
\end{aligned} \tag{3.6}$$

which may be solved to give the refractive indices for the three modes n_1^2, n_2^2, and n_3^2.

Call T_1, T_2, T_3 the electric field amplitude of the three bulk propagating modes, corresponding to the solutions n_1, n_2, n_3 of (3.6). The total internal electric field is

$$\begin{aligned}
&E(x)=\sum_{\alpha=1}^{3}T_\alpha(x)e^{-i\omega t},\\
&T_\alpha(x)=T_\alpha(0)\exp[in_\alpha(\omega x/C)].
\end{aligned} \tag{3.7}$$

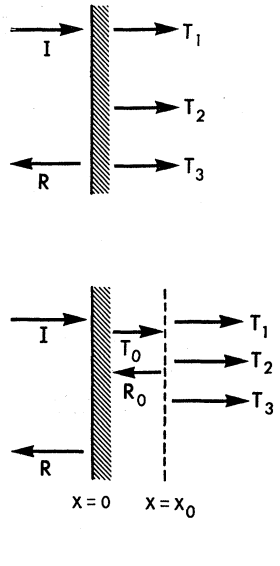

FIG. 3. The electric field amplitudes for three bulk propagating modes; (a) without a surface layer; (b) with a surface layer, the two modes T_0 and R_0 see a dielectric constant ϵ_0.

Once the refractive indices are known, there remains just the boundary problem of matching amplitudes at the surface. The modes for the reflectivity problem are shown in Fig. 3(a). Including the boundary layer from which the polarization wave is excluded,[6] the modes appear as in Fig. 3(b); here, the modes T_0 and R_0 in the surface layer see a background dielectric constant $\epsilon_0=n_0^2$.

Two boundary conditions are needed in addition to the Fresnel condition that E and H be conserved. These are that $P_+=P_-=0$, which applies at the surface layer $x=x_0$, Fig. 3(b). In particular, $P_+=0$ at $x=x_0$ is

$$0=\sum_{\alpha=1}^{3}\frac{T_\alpha(x_0)}{n_\alpha^2-\mu+an_\alpha}.$$

For P_-, replace a by $-a$. The reflectivity is

$$R=\left|\frac{A_1-A_2+in_0(A_1-A_2/\epsilon_0)\tan(n_0\omega x_0/c)}{A_1+A_2-in_0(A_1+A_2/\epsilon_0)\tan(n_0\omega x_0/c)}\right|^2,$$

$$\begin{aligned}
A_1=&-a^2\mu-\mu^2+\mu[n_1^2+n_2^2+n_3^2+n_1n_2+n_1n_3+n_2n_3]\\
&+n_1n_2n_3(n_1+n_3+n_3),\\
A_2=&\mu[n_1^3+n_2^3+n_3^3+n_2^2(n_1+n_3)+n_1^2(n_2+n_3)\\
&+n_3^2(n_1+n_3)+n_1n_2n_3]+n_1n_2n_3[n_1^2+n_2^2+n_3^2\\
&+n_1n_2+n_2n_3+n_3n_1]-(a^2+2\mu)\\
&\times[\mu(n_1+n_2+n_3)+n_1n_2n_3].
\end{aligned}$$

In order to calculate the reflectivity, it is necessary to know the parameters pertaining to the B exciton. These were usually known only approximately. An effort has been made to estimate them realistically; in the end, one would like to have φ the only unknown parameter,

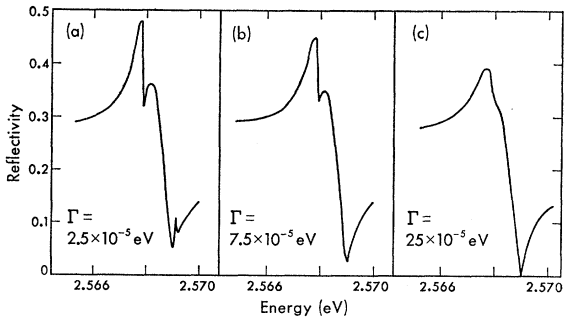

FIG. 4. The theoretical effects of increasing linewidth on 1s B series exciton spectrum for $k\perp z$, $E\perp z$. (a) $\Gamma=2.5\times10^{-5}$ eV, the peak at the longitudinal frequency is present at this small width; (b) $\Gamma=7.5\times10^{-5}$ eV; (c) $\Gamma=2.5\times10^{-5}$ eV, the extra structure is being washed out at increased linewidth.

and to be able to determine it by comparing the calculated and the measured reflectivity curves. The other input numbers and their method of evaluation is outlined below:

1. Resonance frequency. Because of the structure in the reflectivity spectra, the classical Kramers-Kronig version gives the wrong value for the transverse frequency. Calculations with the crossing term included show that in the absence of damping, the low point of the anomalous dip is at this resonance frequency. Damping tends to wash out this minimum, but the measurements indicate that this frequency is 2.5679 eV.

2. Exciton mass. These are derived in the Appendix. The values used in the calculations are $m_{e1}+m_{h1}=1.3$ and $\mu_0=1.7$. The reduced mass turns out to be the same as for the A-series exciton, so that the binding energies and Bohr radius of the two series are roughly equal.

3. Polarizability β. Because of spatial dispersion effects, interpreting the reflectivity curve as a classical spectra gives the wrong value for β. However, it may be predicted by relating it to the polarizability for the $1S$ A-series exciton $\beta(A)$. Assuming that the Bohr radius for the A- and B-series excitons are equal, the two polarizabilities differ only in their band to band matrix element. These may be estimated from (2.5) and

$$\beta(B)=\beta(A)\frac{2}{2+(2-3\lambda_B/\delta)^2}.$$

Since $4\pi\beta(A)=0.0125$;[6] then $\beta(B)=0.00058$. The values 0.00060 and 0.00065 have been used in the calculations. The latter number gives a slightly better fit to the experimental data, but the uncertainty in the other parameters precludes selecting either value as more reasonable.

4. Linewidth. Calculations on the A-series excitons show that the sharp subsidary peak occurs at the longitudinal frequency for linewidths less than 5×10^{-5} eV. Since the B exciton has the same Bohr radius, it should feel the same potential and the reflectivity spectra should show the same peak. Since this is not observed experimentally, the B-series exciton must have a larger linewidth. This is reasonable, since the B state has all of the decay modes of the A state, plus the additional possibility of decaying to the lower energy A state. A rough calculation was made of the decay rate from the B to A state with the spontaneous emission of an acoustical phonon. The main contribution is from deformation potential interaction, and the process contributes a linewidth of the order of 10^{-5} eV, which may account for the increase. Figure 4 shows theoretical reflectivity curves for values of 2.5×10^{-5} eV, 7.5×10^{-5} eV, and 25×10^{-5} eV. The value $\Gamma=7.5\times10^{-5}$ eV is large enough to wash out the subsidary peak, and is used in the remaining calculation.

5. Surface layer thickness. A surface layer of 70 Å was arbitrarily selected for the calculations. The results change little for values of this parameter between 0 and 100 Å, since the effect does not depend upon the presence of the layer.

Using these parameters, φ can be varied to see the effects of the linear crossing on the reflectivity. Figure 5(a) shows $\varphi=0$ (dashed line) and $\varphi=0.3\times10^{-9}$ eV-cm (solid line), while Figs. 5(b) and (c) have 0.5×10^{-9} eV-cm and 0.8×10^{-9} eV-cm. Figure 5(b) represents the experimental curves quite well, so that $\varphi\sim0.5\times10^{-5}$ eV-cm. From the uncertainty of all of the other parameters, the uncertainty on this value may be as high as 50%. The important result is that the presence of such small crossing terms can explain the anomalous features of the reflectivity. Since these have never been measured previously, the fact that they are finite has been established, and a tentative value presented. This value is in agreement with previous theoretical estimates.[4]

The reflectivity can be explained by the presence of the linear crossing term. The main argument which could be made against the explanation is that it is not unique: other forms of band structure could possibly lead to the same reflectivity curves. An identical set of calculations was made on a system which looks quite similar—this is where the bands split quadratically. The two bands have masses m_1 and m_2, and associated with

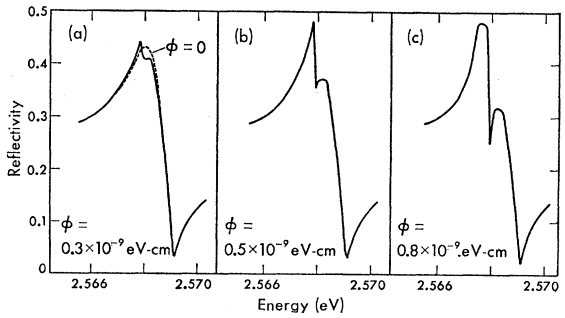

FIG. 5. The theoretical effect of increased linear splitting on the reflectivity spectrum. (a) $\varphi=0$ (dashed line) and $\varphi=0.3\times10^{-9}$ eV-cm (solid line); (b) $\varphi=0.5\times10^{-9}$ eV-cm; (c) $\varphi=0.8\times10^{-9}$ eV-cm. The middle value appears as the most reasonable fit to the experimental data, Fig. 2.

each band is a polarization wave. This system will also have three propagating modes, and the boundary conditions $P_1=P_2=0$ are applied as before. Reflectivity curves were calculated for a wide range of m_1 and m_2, but none led to the type of structure observed experimentally. It is concluded that the linear crossing term must account for the effect.

ACKNOWLEDGMENT

We wish to thank D. G. Thomas for graciously providing the data used in Fig. 2.

APPENDIX

The effective masses of holes in the second valence band, which are needed for the reflectivity calculation, have not been measured. But using a $\mathbf{k}\cdot\mathbf{p}$ perturbation model which relates the three valence bands, the B band masses are estimated from a knowledge of the A band masses. Without this relationship, each band would have the form (2.4) and its own set of independent constants; of course, for Γ_9 bands $C=0$.

The scheme employed to relate the constants for the different masses is to view wurtzite as a strained zincblende material. This model was previously used to estimate oscillator strengths in CdS.[13] By simultaneously introducing the strain and spin-orbit interactions into a sixfold degenerate zincblende valence band, a wurtzite-type structure with the three doubly degenerate bands results. The valence band states which result are those given by (2.5). The masses may be obtained by also introducing the $\mathbf{k}\cdot\mathbf{p}$ perturbation matrix appropriate for zincblende. The linear wave vector terms do not contribute to the masses and are omitted. The most general form for quadratic wave vector terms is

$$\begin{pmatrix} Dk_x^2+Gk^2 & Fk_xk_y & Fk_xk_z \\ Fk_xk_y & Dk_y^2+Gk^2 & Fk_yk_z \\ Fk_xk_z & Fk_yk_z & Dk_z^2+Gk^2 \end{pmatrix}. \quad \text{(A1)}$$

Including spin degeneracy causes (A1) to appear twice in a sixfold representation. One way of finding the masses is to include (A1) in the simultaneous diagonalization of the spin-orbit and strain terms. Although this is possible, the result is not simple enough to be useful. An easier method is to transform the $\mathbf{k}\cdot\mathbf{p}$ perturbation to a matrix with basis states given by (2.5). Since the transformation is linear, the wave vector terms will still be of order k^2 in all matrix elements. The off-diagonal terms are only important when wave vector-dependent mixing of the basis states occurs. This effect may be ignored for small wave vectors, so that the diagonal elements determine the masses. They are

$$A \text{ band}, \quad E_A=\lambda_A+(D/2)(k_x^2+k_y^2)+Gk^2,$$

$$B \text{ band}, \quad E_B=\lambda_B+DN_B^2\{k_x^2+k_y^2+[2-(3\lambda_B/\delta)]^2k_z^2\}+Gk^2,$$

$$C \text{ band}, \quad E_C=\lambda_C+DN_C^2\{k_x^2+k_y^2+[2-(3\lambda_C/\delta)]^2k_z^2\}+Gk^2.$$

Note that the constant F of (A1) does not enter into the band masses. Only two constants, D and G, determine all six masses, and these may be found from the two masses of the top valence band. The perpendicular mass is known,[6] $m_\perp=0.70m$ (m=electron mass), and the parallel mass is estimated $m_\parallel\sim 5m$. The B and C band masses are listed for A-band parallel masses of 3.0, 5.0, and ∞. Define $d=(2m/\hbar^2)D$, $g=(2m/\hbar^2)G$, and the results are listed in Table I.

TABLE I. Masses for the various bands.

Bands	$g=0.333$ $d=2.20$	$g=0.20$ $d=2.46$	$g=0$ $d=2.86$
A band:			
$m_\parallel/m=g^{-1}$	3.0	5.0	∞
$m_\perp/m=(g+d/2)^{-1}$	0.70	0.70	0.70
B band:			
$m_\parallel/m=[g+dN_B^2(2-3\lambda_B/\delta)^2]^{-1}$	0.79	0.81	0.83
$m_\perp/m=[g+dN_B^2]^{-1}$	1.03	1.09	1.20
C band:			
$m_\parallel/m=[g+dN_C^2(2-3\lambda_C/\delta)^2]^{-1}$	0.62	0.62	0.61
$m_\perp/m=[g+dN_C^2]^{-1}$	1.25	1.39	1.65

For excitons from the B valence band, the following parameters may be estimated:

$$\mu_0=0.17,$$
$$m_{e\perp}+m_{h\perp}=1.2\rightarrow 1.4,$$
$$\gamma=10^{-2}.$$

The measure of the anisotropy γ is very small, and the isotropic Hamiltonian approximation is very good.

[13] G. Dresselhaus, Phys. Chem. Solids 1, 14 (1956).